Two-point matrix probability function for two-phase random media: Computer simulation results for impenetrable spheres

J. M. Haile and C. Massobrio

Department of Chemical Engineering, Clemson University, Clemson, South Carolina 29634

S. Torquato

Department of Mechanical and Aerospace Engineering and Department of Chemical Engineering, North Carolina State University, Raleigh, North Carolina 27695

Computer simulation results are reported for the two-point matrix probability function S_2 in two-phase random, homogeneous systems composed of completely impenetrable spheres. The results compare favorably with the earlier analytic predictions of S_2 made by Torquato and Stell.

I. INTRODUCTION

Certain kinds of two-phase random media, such as suspensions, porous media, and composite materials, are characterized by a discrete particle phase that is distributed throughout a continuous matrix phase (fluid, solid, or void). A fundamental understanding of the effective bulk properties of such systems rest upon knowledge of certain statistical quantities that describe how the phases are spatially distributed. In a series of recent papers,[1-5] Torquato and Stell have studied a set of n-point matrix probability functions S_n which provide such a description of the microstructure. Once low-order S_n, such as S_2 and S_3, are known, then effective bulk properties, the diffusion coefficient,[6] thermal conductivity,[7-10] and elastic moduli[10,11] for example, can be estimated by evaluating integrals over these S_n probability functions.

The general n-point function S_n may be interpreted physically as the probability associated with randomly throwing n points into the disordered system such that all n points fall in the matrix phase. The one-point function S_1 is therefore merely the volume fraction ϕ of the matrix. For a homogeneous and isotropic medium the two-point function S_2 depends on both the matrix volume fraction and the relative distance r between the two points randomly thrown into the system. Similarly, the three-point function depends upon the size and shape of the triangle whose vertices are the three, randomly thrown points (r,s,t).

For random media in which completely impenetrable (hard) spheres form the discrete phase, Torquato and Stell[5] have given formal analytic expressions for the two- and three-point functions. These expressions involve integrals over the two- and three-body distribution functions $g_2(r)$ and $g_3(r,s,t)$, respectively, of the impenetrable spheres. Torquato and Stell were able to evaluate the integral for S_2 using the Verlet–Weis[12] modification of the analytic solution[13,14] to the Percus–Yevick equation for the hard-sphere two-body distribution function $g_2(r)$. These computations for S_2 were performed at six values of the matrix volume fraction $\phi = 0.38, 0.5, 0.6, 0.7, 0.8$, and 0.9.

This paper reports what we believe to be the first computer simulation results for any n-point matrix probability function. Molecular dynamics simulations were performed on the hard-sphere system at the matrix (void) fractions studied by Torquato and Stell and the two-point function was evaluated from the resulting hard-sphere trajectories. The theoretical values for $S_2(r)$ are found to be in generally good agreement with the computer simulation results.

II. CALCULATION PROCEDURE

Molecular dynamics simulations were performed on hard-sphere systems using the method described by Alder and Wainwright.[15] The spheres were contained in a cubic volume of side L and periodic boundary conditions were employed. Runs were performed at each of the matrix (void) volume fractions studied by Torquato and Stell and cited above. Each run was started from a face-centered cubic lattice and in each case an initial few thousand collisions were run and discarded before sampling for equilibrium properties was begun. The judgement as to the exact number of initial collisions to discard was based on the mean time between collisions attaining an essentially constant value. An additional 20 000 collisions were then used to form the equilibrium portion of each run. The total energy of the system was conserved to one part in 10^7 over 100 collisions, using double precision arithmetic on an IBM 3081 computer.

We adopted the residual pressure $(P/pkT\text{-}1)$ as a sufficient criterion that the simulations were properly performed. Several methods may be used to evaluate the pressure from hard-sphere simulations.[16] We chose to use the time rate of change of momentum transfer on collision,[17] evaluating the slope of momentum transfer vs time by least squares. The pressures obtained from this procedure were compared with the essentially exact values provided by the Carnahan–Starling[18] equation of state. Using 108 hard spheres we found small but consistent discrepancies between our values and the Carnahan–Starling values for the residual pressure. These discrepancies were presumably a reflection of system-size dependence, because with 256 spheres the discrepancies were almost completely eliminated, as shown in Table I. Hence, the results reported here are for simulations using 256 spheres, except for the $\phi = 0.9$ case discussed below. (The hard-sphere system at $\phi = 0.38$ is a solid and since the Carnahan–Starling equation of state applies only to the fluid phase, no value for the residual pressure is shown in Table I under the Carnahan–Starling heading at this state condition.)

From the equilibrium portion of each run, hard-sphere positions were stored on magnetic tape at intervals of 100 collisions and these 200 sets of positions were subsequently

TABLE I. Summary of simulation results. (The simulation results in columns 3–5 are from runs with 256 hard spheres, except for those at $\phi = 0.9$ which are for 864 spheres.)

Void volume fraction ϕ	$(P/pkT-1)$ CS Eq.[a]	$(P/pkT-1)$ MD	One-point function S_1	rms relative deviation[b] in two-point function S_2
0.38	⋯	17.1	0.3805	0.04
0.60	5.926	5.929	0.6007	0.007
0.70	2.974	2.966	0.7000	0.003
0.80	1.406	1.409	0.8006	0.002
0.90	0.521	0.521	0.9007	0.005

[a] CS = Carnahan–Starling (Ref. 18) equation of state for hard spheres.
[b] Calculated by Eq. (3).

analyzed for the one- and two-point matrix probability functions. The sampling for $S_2(r)$ involved the following procedure for throwing random vectors into the system. For hard spheres of diameter σ, a length r of the vector was chosen from a random, uniform distribution on $[0, 2.5\sigma]$, since the theoretical calculations[5] indicate S_2 always reaches its long-range limit by $r = 2.5\sigma$. Three random numbers uniformly distributed on $[-L/2, +L/2]$ were used for the Cartesian coordinates that located the center of the vector relative to the center of the cube. Three additional random numbers uniformly distributed on $[-1, +1]$ were used as direction cosines for the vector's orientation. A multiplicative congruential method was used to generate all random numbers.[19]

The positions of the endpoints of this random vector were then checked to determine whether they fell within a sphere. If $\mathbf{r}_i$ represents the position vector locating the center of sphere i and $\mathbf{v}$ is the vector (relative to the same origin as used for $\mathbf{r}_i$) locating a randomly thrown point, then the point lies in the matrix phase if

$$|\mathbf{r}_i - \mathbf{v}| > \sigma/2 \quad \text{for all} \quad i = 1, 2, ..., N, \tag{1}$$

where N is the total number of spheres in the system. If either end of the random vector fell out of the cubic container, then a periodic image of that point was used. Likewise the test for overlap (1) of random points with spheres must include sampling of periodic images of spheres immediately adjacent to the container boundaries. Thus, although all sphere centers lie in the cube, those near the boundaries may have portions extending beyond the cube; those portions will be reflected into the system through opposing faces of the cube and may overlap the random point.

The determination of $S_2(r)$ was performed by accumulating a histogram with respect to the length of the random vectors; a mesh size of $\Delta r = 0.1\sigma$ was used here. If both ends of the random vector satisfied the point-sphere nonoverlap condition (1), then the counter $N(r_k)$ for the histogram mesh element r_k satisfying $|r_k - r| < \sigma/2$ was incremented by unity. At the end of the sampling process the counters for each element in the histogram were normalized by the total number of random vectors thrown M, so that

$$S_2(r_k) \approx N(r_k)/M. \tag{2}$$

The approximation in Eq. (2) becomes exact in the limit as the mesh size Δr approaches zero and the total number of sample vectors M becomes large. After several trial calcula-

tions we found that 15 000 random vectors per set of hard-sphere positions gave adequate statistical precision for $S_2(r)$. Thus the sampling of $S_2(r)$ for each state condition utilized a total of $M = 3(10^6)$ random vectors.

If the above procedure is implemented as described and if not only each sphere but also the image closest to the random point is checked for each sphere (rather than checking just the images of those spheres near the boundaries), then the computation time needed to sample for $S_2(r)$ is prohibitively long. About a factor of 8 increase in execution speed can be achieved by using a cell list[20,21] to reduce the number of spheres and images to be tested for the overlap condition (1).

The cell-list method was implemented by first dividing the system volume into cubic cells, each of side $0.95\sigma/\sqrt{3}$, so that at one instant a cell may contain only one sphere center. For each set of sphere positions read from the magnetic tape, we first construct an array that identifies which cells are occupied by spheres. Then for each random point thrown, the overlap condition (1) is tested as follows: (a) Determine which cell is occupied by the random point. (b) Check the sphere array to determine whether a sphere center lies in the same cell. (c) If a sphere center also lies in the cell, test for overlap by condition (1). (d) If overlap occurs, increment the counter on the appropriate histogram element and consider the next random point. Only one sphere has been tested for condition (1) and no periodic images need be considered. (e) If no sphere lies in the same cell as the point or if the sphere does not overlap the point, a sphere in an adjacent cell may partially lie in the cell and hence may overlap the point; therefore, check the 26 immediately adjacent cells for spheres and overlap via steps (b)–(d). (f) If the cell containing the random point or any of its adjacent cells lie on a system boundary, then the possibility of the point being contained within an image sphere must be checked.

This procedure reduces the testing of each random point for overlap from all N spheres to at most 27 spheres. Using this method for systems of 256 spheres, the sampling of the total $3(10^6)$ random pairs of points required about 18.3 min of central processor (CPU) time on the IBM 3081. The molecular dynamics simulation for 256 spheres itself requires about 6.3 min of CPU time to generate 20 000 collisions.

In addition to evaluating S_2, we also determined the one-point function S_1 from the simulation data. This serves as one consistency check on both the simulation and the sampling procedure, since S_1 must be equal to the matrix volume fraction ϕ. Values for S_1 were determined by two methods: In the first method, besides the seven random numbers generated for each random vector sampled for S_2, as described above, three additional random numbers uniformly distributed on $[-L/2, +L/2]$ were used to locate a random point in the system relative to the center of the cube. This point was tested for point-sphere overlap (1) by the cell-list method and a counter for S_1 was incremented by unity if the point was found to be in the matrix phase. A total of $3(10^6)$ points were sampled for S_1 for each hard-sphere state condition simulated.

In the second method no additional random numbers were generated for S_1; rather, the endpoints of the random vectors sampled for S_2 were also used as samples for S_1. The

motivation of this method is that with no additional computational effort over that used for S_2, one accumulates S_1 with twice as large a sampling population as used in the first method.

III. RESULTS

The simulation results for the one-point function are presented in Table I. The results for $\phi \neq 0.9$ were determined by the first method (above) in which the sampling for S_1 was distinct from that for S_2. The tabulated result at $\phi = 0.9$ is from the second method. At the lower matrix volume fractions the coupling of sampling S_1 with S_2 used in method 2 produces a small but discernable bias of about $+0.003$ in the calculated S_1 values, so the results from the first method are more accurate. At the highest matrix volume fraction of 0.9 (low hard-sphere density), this bias in the first method does not appear or at least is overshadowed by the increased sampling population used in the second method, so method 2 is more reliable at that state condition.

The simulation results for the two-point function are compared with the theoretical calculations of Torquato and Stell[5] in Fig. 1. At the intermediate state conditions $\phi = 0.6$, 0.7, and 0.8, the theoretical and simulation results are in excellent agreement. For the $K = 25$ elements of the $S_2(r)$ histogram sampled on $0 < r < 2.5\sigma$, the root mean square relative deviations between the simulation and theoretical values

$$\text{rms Dev} = \left((1/K) \sum \left\{ \left[S_2(r_i)^{\text{MD}} - S_2(r_i)^{\text{theory}} \right] \right. \right.$$
$$\left. \left. / S_2(r_i)^{\text{theory}} \right\}^2 \right)^{1/2} \qquad (3)$$
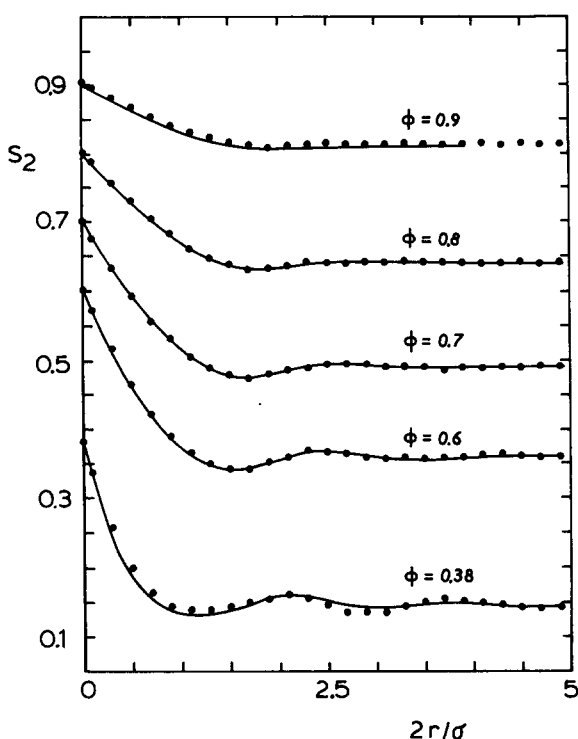

FIG. 1. Two-point matrix (void) probability function for systems of impenetrable spheres. Closed circles are the results from molecular dynamics simulation and lines are theoretical results obtained from quadratic interpolations of the tabulations in Torquato and Stell (Ref. 5). The simulation results are for systems of 256 hard spheres except those at $\phi = 0.9$ which are for 864 spheres. ϕ is the void volume fraction.

are satisfactorily small, as shown in Table I. The values for $S_2(r_i)^{\text{theory}}$ used in Eq. (3) were obtained from quadratic interpolations of the analytic results tabulated in Ref. 5. Both the simulation and theoretical results for $S_2(r)$ exhibit the proper limiting values at small and large r,

$$\lim_{r \to 0} S_2(r) = S_1 = \phi$$

and

$$\lim_{r \to \infty} S_2(r) = \phi^2.$$

The state point $\phi = 0.5$ is very near that at which the hard-sphere system begins to exhibit separation into fluid and solid phases. The system structure obtained in simulations at that density is typically intermediate between fluid and solid; e.g., it may be characteristic of an amorphous glass or it might be a two-phase system with remnants of the solid and fluid interdispersed. Accordingly, simulation results were not obtained for the matrix volume fraction $\phi = 0.5$.

At $\phi = 0.38$ the simulated system was definitely a solid and the resulting two-point function appearing in Fig. 1 shows the most marked structure of any of the state conditions studied. At this packing fraction the theoretical calculations and simulation results yield approximately the same period and frequency of oscillations in $S_2(r)$, but the amplitudes predicted by the theory are smaller than those found in the simulation. This difference in amplitudes is not unexpected because at sphere volume fractions above about 0.5 the Verlet–Weis expression for the hard-sphere $g_2(r)$ more nearly approximates the structure of a glass than a crystal.[5]

The simulation results for $S_2(r)$ were found to be least reliable at the matrix volume fraction $\phi = 0.9$. At this state condition the simulation results for S_2 displayed a significant dependence on the number of spheres used. Runs with 256, 500, and 864 spheres showed rms relative deviations from the theory [Eq. (3)] of 1.2%, 0.72%, and 0.55%, respectively. These deviations vary with the number of spheres N as approximately $N^{-0.65}$.

The 500-sphere result is the average of three runs, the equilibrium portion of each was 40 000 collisions long with sampling for S_2 performed every 100 collisions. To sample different regions of phase space these three runs were separated by runs of 80 000 collisions. That is, at the end of the first (second) run, 80 000 additional collisions were performed before the second (third) run was begun. The $S_2(r)$ results from the three runs were consistently about 1% above the theoretical values, suggesting that the discrepancy is systematic rather than statistical.

A single run was then performed using 864 spheres, with the equilibrium duration 40 000 collisions and sampling for S_2 performed every 100 collisions. The results from this run are those shown in Table I and Fig. 1 for the $\phi = 0.9$ state condition. In Fig. 1 the points from the simulation lie consistently above the theoretical curve, though as cited above, the rms deviation is now about 0.5%.

Two objectives have been met in this work. One is that the simulation results confirm the predictions of the Torquato–Stell theory for the two-point matrix probability function in systems of impenetrable spheres. For fluid state

conditions at which reliable expressions for the hard-sphere two-body distribution function are available (i.e., $\phi > 0.5$), the theory and simulation are in good agreement. For $\phi = 0.38$ the merits of the theoretical calculations cannot be assessed since the glassy state, rather than the ordered solid found in the simulation, was modeled in the theory. Nonetheless, good qualitative agreement exists between the theoretical and simulation results at this high sphere density.

Second is that a viable method has been devised and tested for determining the two-point matrix function from simulation. The method may now be used to evaluate $S_2(r)$ for other models of two-phase random media and thereby help guide further theoretical developments in the description of such systems. Such guidance should prove especially valuable for complex media because rigorous descriptions of such systems pose formidable theoretical difficulties.

ACKNOWLEDGMENTS

[1] S. Torquato and G. Stell, J. Chem. Phys. 77, 2071 (1982).
[2] S. Torquato and G. Stell, J. Chem. Phys. 78, 3262 (1983).
[3] S. Torquato and G. Stell, J. Chem. Phys. 79, 1505 (1983).
[4] S. Torquato and G. Stell, J. Chem. Phys. 80, 878 (1984).
[5] S. Torquato and G. Stell, J. Chem. Phys. 82, 980 (1985).
[6] S. Prager, Physica 29, 129 (1963).
[7] M. Beran, Statistical Continuum Theories (Wiley, New York, 1968).
[8] G. W. Milton, Phys. Rev. Lett. 46, 542 (1981).
[9] S. Torquato and G. Stell, Lett. Appl. Eng. Sci. 23, 375 (1985).
[10] S. Torquato and J. D. Beasley, Intl. J. Eng. Sci. (in press).
[11] S. Torquato, G. Stell, and J. D. Beasley, Lett. Appl. Eng. Sci. 23, 385 (1985).
[12] L. Verlet and J. J. Weis, Mol. Phys. 34, 939 (1972).
[13] E. Thiele, J. Chem. Phys. 39, 474 (1963).
[14] M. Wertheim, Phys. Rev. Lett. 10, 321 (1963); J. Math. Phys. 5, 643 (1964).
[15] B. J. Alder and T. E. Wainwright, J. Chem. Phys. 31, 459 (1959).
[16] W. W. Wood and J. J. Erpenbeck, in Statistical Mechanics, Part B, edited by B.J. Berne (Plenum, New York, 1977), Chap. 1.
[17] B. J. Alder and T. E. Wainwright, Proceedings of the International Symposium on Transport Processes in Statistical Mechanics, edited by I. Prigogine (Interscience, New York, 1958).
[18] N. F. Carnahan and K. E. Starling, J. Chem. Phys. 51, 635 (1969).
[19] D. E. Knuth, The Art of Computer Programming (Addison–Wesley, Reading, MA 1969), Vol. 2, Chap. 3.
[20] J. Kushick and B. J. Berne, in Statistical Mechanics, Part B, edited by B. J. Berne (Plenum, New York, 1977), Chap. 2.
[21] B. Quentrec and C. Brot, J. Comput. Phys. 13, 430 (1973).